Enantioselective hydrogenation of dimethyl itaconate with immobilized rhodium-duphose complex in a recirculating fixed bed reactor

Al-Herz, MA; Tsoligkas, Andreas; Simmons, Mark; Wood, Joseph

DOI:
10.1016/j.apcata.2011.02.009

*Graphical Abstract

Graphical Abstract

ENANTIOSELECTIVE HYDROGENATION OF DIMETHYL ITACONATE WITH IMMOBILIZED RHODIUM-DUPHOS COMPLEX IN A RECIRCULATING FIXED-BED REACTOR

M.A. AL Herz, A.N. Tsoligkas, M.J.H. Simmons, J. Wood

School of Chemical Engineering, University of Birmingham, Edgbaston, Birmingham, B15 2TT

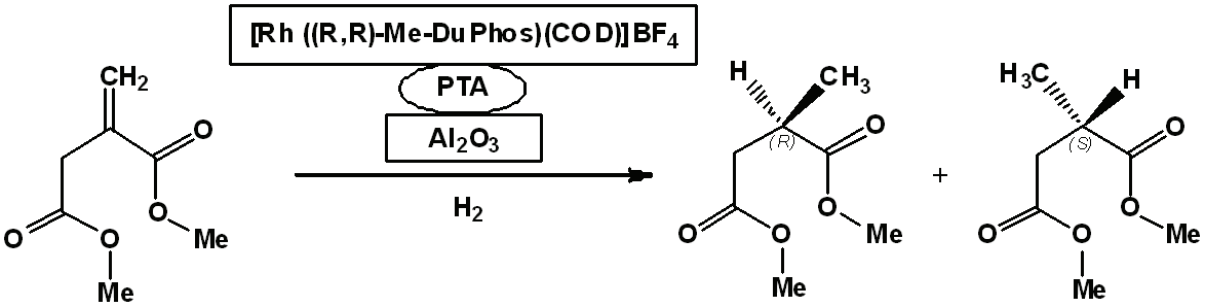

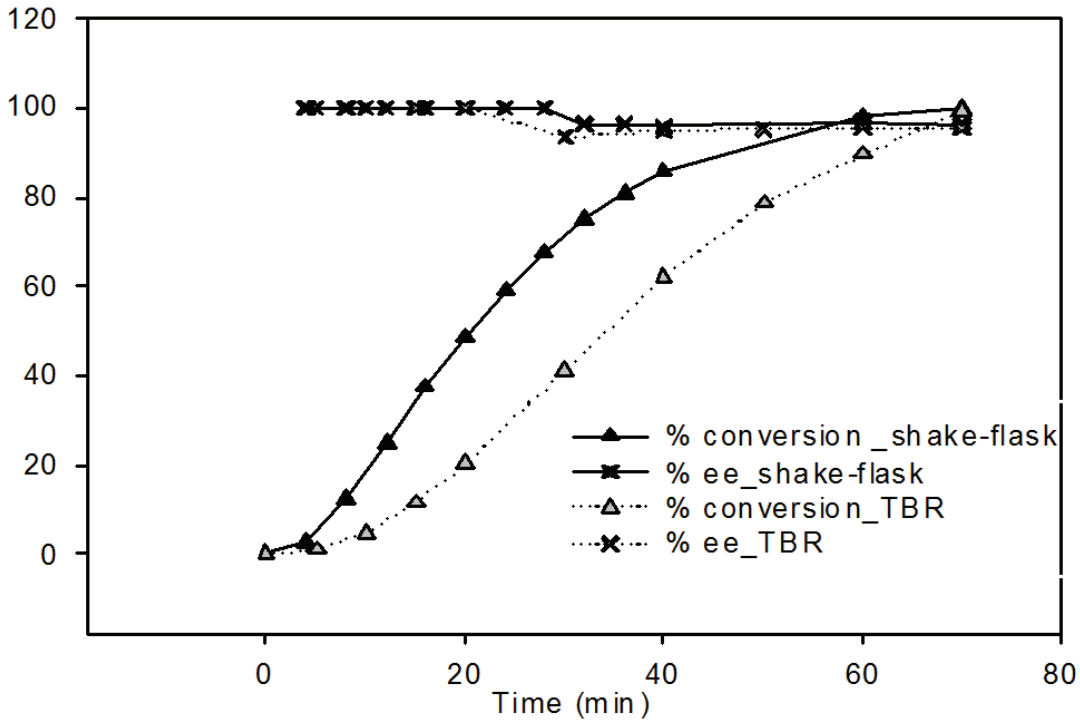

*Research Highlights

- Selectivity of dimethyl itaconate hydrogenation assessed in a trickle bed reactor
- Osborn-Wilkinson kinetics showed complexation before reaction with hydrogen
- Using trilobe alumina support gave high enantioselectivities in the TBR
- Changing hydrodynamics affected both reaction rate and enantioselectivity

ENANTIOSELECTIVE HYDROGENATION OF DIMETHYL ITACONATE WITH IMMOBILISED RHODIUM-DUPHOS COMPLEX IN A RECIRCULATING FIXED-BED REACTOR

M.A. AL Herz, A.N. Tsoligkas, M.J.H. Simmons, J. Wood
School of Chemical Engineering, University of Birmingham, Edgbaston, Birmingham, B15 2TT

Abstract

The catalytic hydrogenation of dimethyl itaconate was studied in lab-scale shake flask and transferred to continuous flow with recirculation in a trickle bed reactor. All experiments were performed under ambient conditions (20^{o}C and atmospheric pressure). The catalyst complex [Rh((R,R)-Me-DuPhos)(COD)]BF_4 was anchored to powder and trilobe alumina supports using phosphotungstic acid (PTA) as an anchoring agent. For the powder alumina, tests were conducted in the shake flask to ensure that the reaction was not influenced by mass transfer limitations by varying the stirrer speed and catalyst mass, thus ensuring the reported data are in the kinetic regime. In the shake-flask [substrate to catalyst molar ratio of 60, atmospheric pressure (101317 Pa), room temperature (293.15 K), H_2 flow rate of 100 ml min^{-1} (1.7×10^{-6} m^3 s^{-1}) and agitation speed of 200 rpm], a turnover frequency (TOF) of 50 h^{-1} (1.4×10^{-2} s^{-1}) was achieved with powder alumina support in comparison to a TOF of 20 h^{-1} (5.6×10^{-3} s^{-1}) obtained with the trilobes. Under these conditions, the enantioselectivities obtained from immobilising the catalyst complex onto the powder and trilobe supports were 96% and 97%, respectively. Fitting Osborn-Wilkinson kinetics to the concentration profiles indicated that complexation with the olefin before reaction with hydrogen was the preferred path. The trickle bed reactor (TBR) was operated in the trickle flow regime using the trilobe support. Optimal gas and liquid flow rates were selected which were found to have a noticeable effect on initial reaction rate and enantioselectivity. Under optimized conditions in the TBR [substrate to catalyst molar ratio of 223, atmospheric pressure (101317 Pa), room temperature (293.15 K), gas flow rate of 100 ml min^{-1} (1.7×10^{-6} m^3 s^{-1}) and liquid flow rate of 20 ml min^{-1} (3.3×10^{-7} m^3 s^{-1})], 99% conversion and enantioselectivity of up to 99.9% were achieved.

Keywords: Anchored homogeneous catalyst; [Rh ((R,R)-Me-DuPhos)(COD)]BF_4; Dimethyl itaconate hydrogenation; shake-flask reactor; trickle bed reactor

1. Introduction

Optically active compounds are the constituents of many medicines, vitamins, flavours, fragrances, herbicides and pesticides. They are also the building blocks of proteins, carbohydrates and DNA which are the principal components of life itself. Baiker [1] demonstrated that research in this field has been driven by the fact that the 'wrong' enantiomer of a chiral product may have negative side effects which outweigh the beneficial value of the 'right' enantiomer, a well known example being birth defects caused by the drug thalidomide. Such cases drive today's emphasis towards production of enantiomerically pure active ingredients.

Enantioselective catalysis is an attractive method of producing a single enantiomer, which has been applied to reactions involving the hydrogenation of carbon-carbon, carbon-nitrogen, and carbon-oxygen bonds [2] with high efficiency and low environmental impact. Moreover,

information on industrial applications of enantioselective catalytic reactions has increased both in quantity and in quality with the enantioselective hydrogenation of olefins being a prime example with industrial relevance [3].

Homogeneous transition-metal-catalyzed asymmetric hydrogenation has attracted increased attention for the production of enantiopure pharmaceuticals and agrochemicals [4]. However, large-scale applications of this mature methodology are hindered by the difficulty of catalyst separation and reuse. To overcome these issues, attention has recently focused on heterogenisation or immobilisation of metal complexes upon supports. Hems *et al*. [5] claimed that poorer enantioselectivities are usually achieved with the immobilised complex when compared to homogeneous catalysts although for some rare cases improved enantioselectivity can occur.

Despite the various well described procedures which allow for the immobilisation of a metal complex onto a solid support, it is still a challenge to synthesize efficient catalysts from these precursors. Once immobilised, the complex must maintain its activity and selectivity, be easily recovered and not leach under the reaction conditions [6]. Among these conflicting requirements, covalently bound catalysts display possibly the broadest scope due to the link stability towards most solvents or additives such as salts or acids and bases [7].

The enantioselective hydrogenation of β-ketoesters to chiral β-hydroxyesters using nickel catalysts and the hydrogenation of α-ketoesters or acids to chiral α-hydroxyesters or acids using platinum catalysts are two of the most feasible methods to result from over 40 years of research [8]. However, the potential of homogeneous catalysts as candidates for immobilisation could be realized through novel methods of attachment to the support. Augustine *et al*. [9] developed a new technique of immobilisation that involves attaching catalytically active complexes to solid supports via heteropoly acids (HPAs). The active complex is attached to the support through the metal atom, delivering "anchored homogeneous catalysts". The attachment can be either covalent between the metal atom of the complex and the HPA or an ion pair with a metal cation and the oxygen anion of the HPA [9]. This type of attachment avoids the use of the ligand which may be prone to leaching. By applying this technique, turnover frequencies (TOFs) of up to 7000 h^{-1} and enantioselectivities of 97% have been achieved for the hydrogenation of dimethyl itaconate (DMI) together with good recyclability [8].

Production of small volumes of enantiopure compounds and fine chemicals in general are delivered on the industrial scale using batch processing. In contrast, production of large volumes of bulk chemicals employs continuous processing, which affords lower plant inventories, lower production and labour costs and greater process control compared with batch plant at the expense of reduced process flexibility [10]. However, due to the expected increase in production volumes of fine chemicals, the replacement of batch plant with continuous [11] is a natural step forward for large scale production of some optically pure compounds [12-14]. Examples of large production volumes of fine chemicals include ibuprofen, a painkiller at 10,000 tonnes/annum (t/a) [15], S,S-aspartame, a sweetener at 14,000 t/a [16] and (R)-mecropol, a herbicide at 14,000 t/a [17].

Hermán *et al*. [18] stated that heterogeneous catalysts are more suitable for use in continuous processes and that chirally modified metal catalysts are the most promising alternatives for large scale production of optically pure compounds. Heterogeneous catalysts are more suitable for use in continuous reactors, since they do not require separation and recycling.

Therefore efficient immobilisation, or heterogenisation, of homogeneous complexes onto supports is a key issue for the transfer of enantioselective synthesis from batch to continuous operation.

Very few examples of use of continuous processes for production of products using enantioselective catalysts appear in the literature. Künzle *et al*. [19] demonstrated the feasibility of continuous enantioselective hydrogenation over cinchona-modified Pt/alumina for some reactants, including ethyl pyruvate, ketopantolactone and 1-phenyl-1,2-propanedione. However, these reactions required a continuous feed of minute amounts of cinchona modifier to maintain enantioselectivity which is a significant drawback. In addition, continuous operation was found to require higher cinchona alkaloid/reactant ratios to achieve good enantioselectivity compared with the batch reactor [20]. Besides, the catalyst used was in the form of very small particles leading to high pressure drop which is not ideal for fixed bed operation.

In an attempt to tackle high pressure drop across the catalyst bed, Toukoniitty *et al*. [21] studied the enantioselective hydrogenation of 1-phenyl-1,2-propanedione in a fixed bed reactor using knitted silica fiber support material impregnated with platinum. In their work, the modifier was continuously fed to the reactor; the initial enantioselectivity of 23% was extremely low but it increased to a steady state value of 57%.

A significant challenge in assessment of the effectiveness of immobilised homogeneous catalysts for continuous processing at the laboratory scale is the low conversion achieved per pass within the fixed bed. This can be overcome by closed loop operation by recirculation of the reactant/product mixture. Indeed, the application of a closed-recycling configuration has been found to be useful in various research studies [22-24] offering advantages such as achieving high conversions of substrates through prolonged exposure to the catalyst within the fixed bed. This type of operation has also been found applicable to small volume fine-chemical heterogeneous catalytic liquid-phase reactions, as it ensures efficient saturation of hydrogen in the recycling mixture [24].

In this paper, the hydrogenation of dimethyl itaconate (DMI) in a recirculating fixed bed reactor is reported for the first time. DMI reacts with hydrogen to form two isomers as products namely, dimethyl (S)-(-)-methylsuccinate and dimethyl (R)-(+)-methylsuccinate (Scheme 1). The incentive for studying DMI hydrogenation is the importance of succinnic acid derivatives as valuable intermediates for several pharmaceutical preparations including potent renin inhibitors [25].

The objective of this study is to demonstrate that enantioselective hydrogenation of DMI can be performed in a trickle bed reactor using a supported homogeneous catalyst based on an Rh-complex, which does not require a modifier to induce enantioselectivity. For this purpose, the catalyst precursor complex, [Rh ((R,R)-Me-DuPhos)(COD)]BF_4, which is a proven catalyst for this reaction, was immobilised on powder and trilobe alumina supports, following Augustine *et al.* [9]. Comparisons are drawn between powder and trilobe alumina supports used in shake flask reactions with the performance of trilobes in the trickle bed. Conditions have been optimised to maximize the turn over frequencies (TOFs) and an Osborn-Wilkinson kinetic model was fitted to concentration versus time profiles of DMI. In the TBR, reactions were carried out by continuously recirculating the mixture (DMI in EtOH) through the catalyst bed. Based on the results obtained, the possibility of operating in a continuous flow with single pass was evaluated. To achieve optimum conditions in the recirculating mode, the

catalyst loading was optimized and the effect of hydrodynamics (gas and liquid flow rates) upon the performance of the catalytic system as well as the wetting efficiency of the catalyst bed was investigated. All experiments were performed under ambient conditions (20^{o}C and atmospheric pressure), maintaining "green" processing principles. While some previous reports [26, 27, 28] have related the effect of liquid phase hydrogen concentration on ee, the present work aims at a more quantitative assessment of mass transfer effects.

2. Experimental

2.1 Catalyst Preparation

2.1.1 Materials

All chemicals and solvents used in these studies are shown in Table 1. Both powder and trilobe alumina supports were washed with ethanol before use in order to remove fine particles. All solvents (Analytical reagent grade, Fisher Scientific, UK) were degassed by bubbling nitrogen through for several hours before use.

2.1.2 Preparation of Rh ((R,R)-Me-DuPhos)/PTA/Al_2O_3

The preparation procedure of Augustine *et al.* [9] was followed to prepare the catalyst complex. 9 g (9×10^{-3} kg) of alumina was placed in a glass flask and washed 4 times with 50 ml (5×10^{-5} m^3) portions of EtOH. 75 ml (75×10^{-6} m^3) of EtOH (95%) was added to the flask. 1.95 g (1.95×10^{-3} kg) of phosphotungstic acid (PTA) was dissolved in 25 ml (25×10^{-6} m^3) of 95% EtOH and the solution was added drop-wise to the well agitated alumina solution. The mixture was then shaken for a further 4 h. After the reaction liquor was removed, the Al_2O_3/PTA was washed 3 times with 50 ml (5×10^{-5} m^3) portions of EtOH and re-suspended in another 75 ml (75×10^{-6} m^3) of EtOH. A solution of 0.012 M (0.012×10^{3} mol m^{-3}) of [Rh ((R,R)-Me-DuPhos)(COD)]BF_4 in 50 ml (5×10^{-5} m^3) of EtOH was prepared and added drop-wise to the Al_2O_3/PTA and then shaken overnight. The liquor was then removed and the resulting Rh((R,R)-Me-DuPhos)/PTA/Al_2O_3 was washed with 50 ml (5×10^{-5} m^3) portions of EtOH until the wash liquid became colourless.

2.2 Catalyst Characterization

Data on BET surface area, pore size and pore volume of the powder and trilobe supports is given in Table 2. BET surface areas and pore volumes were determined from nitrogen adsorption and desorption isotherm data obtained at 77.3 K on a constant-volume adsorption apparatus (Micromeritics, ASAP-2010). The pore volumes were determined at a relative pressure (P/P_0) of 0.99. Notably, the BET surface area of the powder is almost double that of the trilobe support, with the average pore size within the trilobes being slightly over twice that of the powder support.

2.3 Catalytic Test

2.3.1 Experimental equipment

2.3.1.1 Shake-flask reactor

The experiments were carried out in a 100 ml (100×10^{-6} m^3) Erlenmeyer flask. After transferring the catalyst, solvent and substrate into the reactor, it was sealed with rubber septa. The reactor was then fixed onto the shaking plate of the agitator using adhesive tape. The hydrogen (H_2) flow was set at the desired rate using a flow meter and was then fed into the reactor through a needle attached to a rubber tube. A continuous flow of H_2 was applied to the reactor by venting the gas through another needle inserted into the rubber septa.

2.3.1.2 Trickle bed reactor (TBR)

The schematic diagram of the TBR is shown in Fig. 1. The bed was of 6 mm diameter with a total height of 100 mm. The catalyst was loaded into the reactor to a depth of 95 mm and topped with a 5 mm layer of glass beads to ensure good contact between gas and liquid before entering the bed. H_2 and liquid flows were set at the desired rates using a flow meter and a pump, respectively. Both gas and liquid were admitted simultaneously into the Y-shape mixer before entering the catalyst bed. At the bottom of the reactor, gas was vented and liquid was recycled back to the top of the reactor via the pump, thus forming a recirculating flow through the bed.

All catalyst preparations were made under an inert atmosphere of nitrogen and this inert atmosphere was maintained until the start of the reaction when the inert gas was replaced by H_2.

2.3.2 Hydrogenation tests

2.3.2.1 Catalytic hydrogenations in the shake-flask reactor

The amount of catalyst support used was adjusted to provide 20 μmol (20×10^{-6} mol) of catalyst precursor complex upon the desired support, which was then placed in the flask. The required weight of DMI corresponding to the desired turnover number (TON) was dissolved in 15 ml (15×10^{-6} m^3) of EtOH and the solution was added to the flask. After sealing the top of the flask with septa it was taken off the inert atmosphere and put on the agitator. H_2 was bubbled into the reactor for five minutes to ensure a full displacement of N_2. The orbital agitator was then started by setting the controller at the desired speed. Samples of 40 μL (40×10^{-9} m^3) volume were taken at regular intervals using a syringe and analyzed by GC.

To ensure that the rates of reaction obtained were representative of the reaction kinetics and not influenced by mass transfer, two checks were made. Firstly, the dependence of initial reaction rate on the speed of agitation was investigated and the optimal TOF was detected by optimizing the concentration of DMI.

Secondly, to identify the presence of rate limiting resistances, the mass of immobilised catalyst precursor complex [Rh((R,R)-Me-DuPhos)(COD)]BF_4, m, was varied and the corresponding rate of reaction was measured. Using the following rate expression, [29]

$$\frac{C_i}{R_A} = r_b + \frac{1}{m} r_{cr} \quad , \tag{1}$$

a plot of C_i/R_A versus $1/m$ enables the resistance to gas adsorption, r_b and the combined resistance to internal and external diffusion for the catalyst, r_{cr}, to be determined.

2.3.2.2 Catalytic hydrogenations in the TBR

To achieve acceptable pressure drop in the TBR, trilobe-shaped alumina pellets were used as the powder was found to be unsuitable. The reactor was packed with 20 μmol (20×10^{-6} mol) of catalyst precursor complex immobilised into 2.7 g (2.7×10^{-3} kg) of trilobe alumina. The hydrogenation was begun by setting the H_2 and liquid flows at the desired rates. The effect of catalyst loading was investigated by varying the amount of immobilised complex over 2.7 g (2.7×10^{-3} kg) of trilobe alumina. TON was optimized by testing different concentrations of DMI in 15 ml (15×10^{-6} m^3) EtOH. The influence of changing the hydrodynamics were investigated by testing gas flow rates of 50, 100 and 200 ml min^{-1} (0.83×10^{-6}, 1.7×10^{-6} and 3.3×10^{-6} m^3 s^{-1}) and liquid flow rates of 10, 15 and 20 ml min^{-1} (1.7×10^{-7}, 2.5×10^{-7} and 3.3×10^{-7} m^3 s^{-1}).

2.3.3 Sampling method

Samples of 40 μL (40×10^{-9} m^3) were taken at regular intervals throughout the course of the reaction for GC analysis (Varian GC Model, 30m × 0.25mm × 0.25μm film thickness Gamma DEX™ 225 Capillary Column, injection port: 175 ^{O}C; detector: 180 ^{O}C; column oven: initial temperature 80 ^{O}C, ramp at 3^{O}C/min to 140^{O}C/min, head pressure 15 psig, split ratio −90/1).

To check the reproducibility of results, experiments were carried out in triplicate and the obtained relative experimental error was about 5%.

The enantioselectivity (ee) of the reaction was determined as the enantiomeric excess defined as (S – R)/(S + R).

3. Results and discussion

3.1 Reactions in the shake-flask reactor

3.1.1 Base case

Reactions conducted in lab-scale shake-flask reactor were taken as base cases for comparison with the TBR; an initial substrate to catalyst ratio of 9 was selected as a basis for optimization (Table 3). At this condition, a TOF of about 9 h^{-1} (2.5×10^{-3} s^{-1}) and ee of 97% were obtained. The rotational speed (rpm) of the agitator affects mixing and thus mass transport between gas-liquid and liquid-solid. This was quantified in terms of the dependence of initial reaction rate on the speed of agitation. As shown in Fig. 2, the initial reaction rate increased with an increasing speed of agitation up to 200 rpm, after which it was independent of agitation speed. Therefore, all experiments were conducted at 200 rpm to eliminate external particle mass transfer resistance as a limiting factor for the powdered catalyst. The impact of other mass transfer resistances upon the results is discussed in §3.1.3.

3.1.2 Influence of the substrate concentration

The TOF of 9 h^{-1} (2.5×10^{-3} s^{-1}) was relatively low compared with the the values of 4000-7000 h^{-1} reported by Augustine *et al*. [8], and the values of 2000-19000 h^{-1} reported by Brandts *et al*. [30]. However, these high TOFs were achieved by conducting reactions in an autoclave at H_2 pressures between 3.3×10^5 and 6.6×10^5 Pa and/or temperatures of up to 323.15 K, whilst the results presented here were taken at ambient conditions. Higher pressures and temperatures would be expected to increase H_2 solubility in the liquid phase as well as increasing the rate of reaction.

In order to scale up such processes for application in industry it would be desirable to achieve high TOFs, such as observed by Augustine *et al.* [8] and Brandts *et al*. [30]. However in practice issues concerning catalyst stability, deactivation pathways, reaction kinetics and mass transfer effects could each play a part in causing a lower TOF to be observed. This paper systematically investigates these effects in order to elucidate the limitations of carrying out enantioselective hydrogenations in the shake-flask and trickle bed reactor and suggests possible ways in which they may be overcome.

Among several methods of immobilising catalyst complexes upon a support, each may have advantages and disadvantages. The catalysts used by Brandts *et al*. [30] were prepared following a procedure in which the cationic metal – precursor $[Rh(COD)_2]BF_4$ was first immobilised into γ-alumina followed by a modification of (R,R)-MeDuPHOS. Brandts *et al*. [30] claim that such immobilisation tends to give better reproducibility results in terms of activity and leaching stability. However the method of Augustine in which the catalytic species is attached to the support through the metal atom of the complex via a heterpoly acid as the anchoring agent offers the advantage that it does not lead to modification of the chiral ligand. Thus the immobilised ligand is expected to have the same functionality as the homogeneous complex, resulting in a high enantioselectivity as was observed in the base case of 97 % ee in this work.

Augustine *et al*. [8] pointed out that many previously reported asymmetric hydrogenations were carried out at substrate to catalyst ratios (turnover numbers (TONs) with all of the reaction going to completion) near 100 and therefore an important goal is to increase the ratio

to values which are more commercially significant. They reported with TONs in the range 1000-50000, together with a high rate or TOF [8]. TOFs are expected to vary with the reaction TONs and thus the substrate concentration. Therefore optimisation of the TOF in the current study was carried out by changing the DMI concentrations. The results, given in Table 3 for the powder alumina support, show that the initial reaction rate increased with increasing concentration of DMI. The rate reached its maximum at a substrate to catalyst ratio of 196 after which it dropped to half this value at substrate to catalyst ratio of 311. For substrate to catalyst ratios between 9 and 122 the ee was 96 - 97% and dropped to ~94% at the highest substrate to catalyst ratios of 196 and 311. It is noteworthy that the optimum turnover frequency (TOF) of 99 h^{-1} (2.8×10^{-2} s^{-1}) is still quite low when compared to the above reported literature values, but nevertheless the optimisation shows an order of magnitude improvement.

3.1.3 Determination of mass transfer effects.

Due to the relatively low TOFs observed, investigations were carried out to determine whether the reaction is limited by external mass transfer at the catalyst particle or diffusional limitations within the catalyst pores.

Fig. 3 shows a plot of C_i/R_A versus $1/m$, and according to the straight line form of equation (1) the value of the gas bubble resistance r_b was determined from the intercept and the catalyst resistance r_{cr} from the slope of the line. The catalyst resistance incorporates combined resistance to internal diffusion, reaction, and external diffusion. From Fig. 3 it can be deduced that the catalyst resistance was greater than the gas bubble resistance at the conditions implemented in the reactions, since the line passes almost through the origin, showing negligible value of the intercept. Since the external mass transfer resistance was already determined to be negligible in § 3.1.1, the role of internal mass transfer resistance in the catalyst pores was evaluated by calculating the internal effectiveness factor, which was estimated for the trilobe from the expression for a spherical catalyst particle [29]:

$$\eta = \frac{3}{\phi_1^2} (\phi_1 \coth \phi_1 - 1) \quad (2)$$

Where for a cylindrical catalyst pellet:

$$\phi = (R/2) \sqrt{k_1 S_a \rho_c / D_e} \quad (3)$$

In calculating the value of the Thiele Modulus, ϕ, the intrinsic rate constant was taken from the value determined for powder supported catalyst, which is not subject to internal diffusion limitation. The value of the effectiveness factor for the pellets, η was found to be in the range 0.98 – 1, and therefore the catalyst is not subject to internal diffusion limitations. Consequently, under the experimental conditions employed, all diffusional resistances (inter particle and intra particle) are not rate limiting and therefore it was possible to detect true kinetics from the experimental observations.

3.1.4 Kinetics

Since the reaction between DMI and hydrogen is a bimolecular reaction involving the catalyst complex immobilised upon the catalyst surface, possible kinetic schemes must allow for the formation of intermediate complexes between these reactants and the catalyst surface.

Table 3 shows a strong dependence of the initial reaction rate on the substrate concentration, suggesting that the substrate concentration has a significant effect of the rate. However the possible role of hydrogen concentration upon the rate of the insertion step must also be considered. The dependence of the rate on the substrate concentration and on the contact between the catalyst and the substrate are reflected on the kinetic model introduced by Osborn *et al*. [31] and is shown in Scheme 2.

The rate determining step in this model can be either one or both of two possible paths: (1) attack of uncomplexed olefin on the dihydrido-complex at the vacant site giving a transition state in which both hydrogen and olefin are bound to the metal; (2) attack of molecular hydrogen on the olefin complex leading to the same transition state.

The rate according to the mechanism of Scheme 2 can be expressed by the following equation [31]:

$$R = -\frac{d[S]}{dt} = \frac{(k'K_1 + k''K_2)p[S][A]}{1 + K_1p + K_2[S]} \tag{4}$$

Although this kinetic model is valid for a dissolved complex in liquid phase, its resemblance to Langmuir-Hinshelwood and Eley-Rideal kinetic models proposed for heterogeneous catalysts [29, 32], was the incentive for utilizing it in our work. The assumed elementary steps for the above model are also incorporated in Langmuir-Hinshelwood kinetics, which involve adsorption, surface reaction and desorption phenomena for reactions involving either single- or dual-site mechanisms [29]. Accordingly, equation (4) was regressed to the experimental data at four different initial DMI concentrations using the least squares method. The fit of the experimental results to model curves is shown in Fig. 4. Table 4 shows the corresponding fitted values of the constants in equation (4).

As can be seen in Table 4, the value of the equilibrium constant K_2 is much greater than that of K_1, meaning that the formation of the olefin complex is favoured. Osborn *et al*. [31], using $RhCl(PPh_3)_3$ homogeneous catalyst, obtained the same conclusion after investigating the effect of the admission of hydrogen on the colour of a benzene solution containing the olefin(ethylene)-complex, and the effect of the reversed procedure, which is the admission of the olefin into a benzene solution containing the dihydrido-complex. In the former case, the solution maintained its bright yellow colour, which is a hallmark of the olefin complex. In the latter case, admission of ethylene resulted in a small rapid absorption and the solution again assumed the yellow colour of the olefin complex. Therefore, it was concluded that this was an indication that the olefin complex could not activate molecular hydrogen and hence in their kinetic studies k'' was assumed to be zero. The finding is in agreement with that found for the catalytic hydrogenation of DMI in a biphasic cyclohexane-water system and in a [Triton X-100/1-pentanol]/cyclohexane/water microemulsion using the water-soluble catalyst complex Rh-TPPTS [33]. However, the value obtained for k'' in this work, although very low, was not zero designating some activation of molecular hydrogen which might be due to

the nature of the immobilised catalyst complex giving different interactions with hydrogen molecules. Moreover, this could also be a result of the high value of the equilibrium constant K_2 shifting the reaction toward path (2). The presumed high adsorption of DMI into the catalyst surface, as well as into the vacant sites of powder alumina support, could lead to diminished uncomplexed DMI, resulting in zero value of k' as shown in Table 4.

3.1.5 Influence of the type of support

For the purpose of comparing the effectiveness of the trilobe alumina with the alumina powder, a reaction was carried out in the shake-flask reactor using [Rh((R,R)-Me-DuPhos)(COD)]BF_4 immobilised onto trilobe alumina and the results are shown in Fig. 5 and Table 5. As expected, the reaction rate when the complex was immobilised onto powder alumina was higher than when it was immobilised onto trilobe alumina. This could possibly be attributed to mass transfer limitations in the pellets as well as the larger surface area provided by powder alumina particles, offering BET surface areas of 258 $m^2\ g^{-1}$ for the powder compared with 149 $m^2\ g^{-1}$ for trilobe, as shown in Table 2.

The experiments conducted in the shake-flask reactor made it possible to assess the efficiency of the implemented immobilisation procedure under well controlled conditions. Furthermore, the optimized TON and TOF serve as a basis for comparisons with the TBR.

3.2 Reactions in the trickle bed reactor (TBR)

In this section results for the TBR are presented and compared with those obtained in the shake flask for powder and pellets. Thereafter kinetic modelling of reactions in the TBR and optimisation of hydrodynamic conditions are presented.

Depending on the gas and liquid flow rates and the physical properties of the liquid, various flow regimes may exist in the TBR. Consequently, knowledge of this is important in understanding the hydrodynamics and mass transfer characteristics.

At low liquid rate, the flow pattern is defined as 'trickling', where the liquid trickles over the packing in a laminar flow. As a result, liquid and gas flow rates were initially set at 20 and 100 ml min^{-1} (3.3×10^{-7} and 1.7×10^{-6} $m^3\ s^{-1}$), respectively based on Baker flow map in order for the reaction to fall in the trickle flow regime [34]. Fig. 6 shows a comparison between the trickle-bed reaction at these conditions and the results from the shake-flask. After 16 min reaction time, the initial reaction rates in the trickle-bed and shake-flask reactors were 0.0017 mol l^{-1} min^{-1} and 0.0019 mol l^{-1} min^{-1}, respectively. Although the initial reaction rate was faster in the shake-flask reactor, both reactors achieved high conversions of > 99% and ee of ~96% after 70 minutes. The difference in reaction rates could be due to the suspension of the catalyst particles in the shake-flask resulting in higher intraparticle diffusion and hence a more efficient utilization of the catalyst. Frequent problems in packed bed reactors such as non-uniform flow distribution with flow channelling could have caused concentration gradients affecting the performance of the TBR [35].

3.2.1 Effect of catalyst loading

In order to achieve the optimum complex to support ratio in the catalyst bed, two different catalyst loadings upon the support were tested in the TBR and the results are summarized in Table 6. A conversion of 70% with 80% ee was achieved when a catalyst loading of 12.2 ×

10^{-3} kg complex/kg support was used. However, when the loading was decreased to 4.4×10^{-3} kg complex/kg support, 99% conversion with 95% ee was obtained with a four-fold increase in reaction rate.

The effect of catalyst loading can be explained by the *site isolation theory* presented by Pugin [36]. Isolated sites are those attached to the support in sufficiently low density that they do not interact with each other, and thus are able to maintain their activity and selectivity. In contrast, if the complexes are packed onto the support too densely, they have a strong tendency to react irreversibly with each other, forming dimers that are no longer active. Pugin [36] developed a mathematical rate model on these bases which matched very well with their experimental data.

3.2.2 Influence of the substrate concentration

As was performed for the powder support, it is desirable to increase the TON and TOF with regard to possible commercial application for the trilobes. Different concentrations of DMI were investigated in order to optimize these parameters using substrate to catalyst ratios of 85, 128, 179 and 223 as shown in Table 7. In addition, the catalyst was re-used by performing up to three reactions with the same catalyst to assess if any loss of activity was observed. The recyclability tests were conducted for the lowest and highest substrate to catalyst ratios implemented in this study. For a substrate to catalyst ratio of 85, a slight decrease in initial reaction rate and conversion when going from first to second cycle was observed while ee was maintained at about 96%. However, when going from second to third cycle, the initial reaction rate plummeted to almost quarter of its initial value accompanied by a substantial drop in conversion, from 97% to 17%, while a very high ee of 99.9% was obtained. This very high ee is expected for the very low conversion achieved since the decrease in ee with increasing conversion is well known [e.g. 37, 38].

Possible reasons for catalyst deactivation are polarity of solvent, catalyst poisoning and adsorption of reactants and/or products into the catalyst. Brandts *et al.* [30] focused on the possibility of leaching of the complex from the support when using alcoholic solvents. Leaching of the Rh complexes was found to decrease from MeOH > EtOH > isopropyl alcohol whilst in cyclohexane no leaching was observed [30]. In this study, a Sheldon test was performed to check for leaching [39]. The reaction liquors of the first and second cycles were separated from the support by filtration. Then, an amount of DMI that gave the corresponding substrate to catalyst ratio was added to the solution and reaction was started by bubbling hydrogen through. After running reactions for about an hour, no changes in the products concentrations were observed, and hence it was concluded that no catalytically active complex could have leached from the support. Another possible reason for deactivation may be partial oxidation of the catalyst precursor complex due to some inevitable exposure to air during sampling for GC analysis.

Table 7 also shows that as expected, reaction rate increased with increasing concentration of DMI, as more molecules would be available to occupy the catalytic sites for reaction. The best results were obtained with the highest ratio of 223 giving conversion and ee of 99% and 99.9%, respectively. However, there was again a notable loss of activity upon recycling of the catalyst, with a halving of the rate and drop in conversion to 52% while ee decreased to 94%. Again, application of the Sheldon test showed no presence of leached active complex.

The Osborn-Wilkinson kinetic equation (4) was again fitted to the experimental data obtained from the TBR as shown in Fig. 7. Rate and equilibrium constants are displayed in Table 4. While the value of K_2 is the same for both reactors (Table 4), the values of K_1 and k'' obtained for the TBR are larger. This possibly indicates increased complexation of hydrogen with the catalyst, which could be due to a better mixing of gas and liquid at the top of the TBR resulting in more hydrogen molecules available to complex with the catalyst and to attack the olefin-complex.

3.2.3 Influence of the hydrodynamics

In the TBR, maintaining effective contact of the gas and liquid with the catalyst active sites becomes a significant design consideration in comparison with the well mixed shake flask reactor. Therefore investigation of the hydrodynamics within the TBR is vital for evaluating the performance of the reactor. A suitable selection of gas and liquid flow rates is crucial when basic phenomena such as wetting efficiency of the catalyst bed and mass transfer are evaluated. Therefore, the effect of gas and liquid flow rates on the rate and selectivity of the reaction is discussed in the following sections.

3.2.3.1 Effect of gas flow rate

The results obtained from testing different gas flow rates are shown in Table 8 and the conversion profiles are shown in Fig. 8. Increasing hydrogen flow from 0.83×10^{-6} to 1.7×10^{-6} m^3 s^{-1} increased both reaction rate and enantioselectivity. However, increasing hydrogen flow from 1.7×10^{-6} m^3 s^{-1} to 3.3×10^{-6} m^3 s^{-1}, although increasing the initial reaction rate, decreased overall reaction rate and led to a decrease in enantioselectivity from 99.9 to 94%. Increasing the gas velocity may have led to a decrease in the thickness of liquid film upon the catalyst due to the drag force of gas flowing through the void space. In turn this could have led to a lower liquid hold up and hence decreased residence time of liquid, which would explain the lower reaction rate. However, it is interesting to observe that as gas flow rate was increased from 1.7×10^{-6} m^3 s^{-1} to 3.3×10^{-6} m^3 s^{-1} the flow regime approached pulsed flow. Ramachandran and Chaudhari [34] reported that the transition from trickle to pulse flow is generally characterized by a sharp increase in the root mean square pressure fluctuation for a small increase in gas or liquid flow rate. Owing to the higher interaction between the gas and liquid phases in the pulsing regime some workers have sought to induce pulsing by cycling the liquid feed on and off [40, 41]. Wilhite *et al*. [40] found that this approach was not effective for a system under mild gas limitation as better performance is achieved in steady flow. In contrast Boelhouwer *et al*. [41] found that periodic pulsing operation led to an improvement of 400 % in reaction rate for the hydrogenation of α-methyl styrene. However in the study reported here, it appears that operation in steady flow at lower gas flow rate leads to higher liquid hold up and residence time, in turn giving higher reaction rate and enantioselectivity. Künzle *et al*. [20] reported that enantioselectivity is influenced by the competitive adsorption of all reaction components and possibly some impurities. Therefore, a general positive or negative correlation between hydrogen flow and enantioselectivity cannot be expected, thus explaining the lower enantioselectivity observed at high gas flow rates in this work.

3.2.3.1 Effect of liquid flow rate

The results obtained from investigating different liquid flow rates are summarized in Table 8 and the conversion profiles are shown in Fig. 9. The initial reaction rate and enantioselectivity increased with increasing liquid flow rate with the optimum enantioselectivity obtained at liquid flow rate of 3.3×10^{-7} m^3 s^{-1}.

The wetting efficiencies were calculated based on a correlation developed by Lebigue *et al.* [42]:

$$f = 1 - \exp[-1.986 {Fr_L}^{0.139} {Mo_L}^{0.0195} \square_B^{-1.55}] \quad (5)$$

The correlation uses a bounded function and only three dimensionless groups (liquid Froude and Morton numbers and bed porosity) and has been shown to predict wetting efficiency with very good precision [42].

Mass transfer coefficients were calculated using a correlation by Winterbottom *et al*. [43] for the transport of hydrogen from bulk liquid-to-solid interface:

$$Sh' = 0.266 Re_l^{1.15} Sc^{1/3} \quad (6)$$

A value for the diffusivity of hydrogen into ethanol required for calculation of the Sherwood (Sh) and Schmidt numbers (Sc) was obtained using [44]:

$$D = (1.173 exp^{-16} \emptyset_B^{0.5} M_B^{0.5} T)/\mu V_A^{0.6} \quad (7)$$

The increase in initial reaction rate with liquid velocity could be explained by the improved wetting efficiency and mass transfer coefficient accompanying the increase in liquid superficial velocity as demonstrated in Table 9. High liquid velocities in TBRs result in the catalyst particles being completely covered by the liquid reactant, and the gaseous reactant must penetrate the liquid film for the reaction to take place. However, at low liquid velocities, the surface of the catalyst might not be fully covered by liquid giving a chance for the gaseous reactant to enter into the liquid filled pores through the dry regime without any liquid film resistance. In this case, as the liquid flow rate is increased, the wetting efficiency increases. For gas limited reactions, an increase in wetting efficiency increases the resistance to the transfer of the gaseous reactant from the gas phase to the catalytic sites [45]. This results in a decrease in the overall rate of reaction even though the liquid-solid mass-transfer coefficient increases [46]. However, since the wetting efficiencies obtained from the investigated liquid flow rates are high, as shown in Table 9, and because reactions were not gas limited, the only resistance remaining is the transport of gas from bulk liquid-to-solid interface, Therefore, an increase in liquid flow rate increases mass transfer coefficient which in turn increases reaction rate.

Although high enantioselectivities were maintained throughout the optimization studies, the TONs and TOFs are relatively low compared to what has been achieved by this catalyst [8, 30] at higher temperatures and pressures. Therefore, for the operation in continuous flow with a single pass to be feasible, further optimizations are required. To achieve high TONs and TOFs, further parameters such as temperature, pressure and solvent effects, which have been found to have a remarkable effect upon the performance of the catalyst, need to be carefully examined.

4. Conclusions

The enantioselective hydrogenation of DMI, over [Rh((R,R)-Me-DuPhos)(COD)]BF_4 supported on trilobe alumina, can be successfully carried out in a trickle bed reactor to produce dimethyl (S)-(-)-methylsuccinate. The catalyst gave high enantiomeric excesses in the TBR with results comparable to those obtained in the shake flask batch reactor. After elimination of all diffusional resistances, the experimental data could be fitted well by means of a kinetic model based on the Osborn-Wilkinson reaction mechanism. Applying Osborn-Wilkinson kinetics to the reaction indicated that complexation with the olefin before reaction with hydrogen was the preferred path. Initial reaction rate and enantioselectivity in the TBR could be promoted by optimizing liquid flow rate which was found to be directly proportional to wetting efficiency of the catalyst bed as well as mass transfer of H_2 from bulk liquid to catalyst surface.

Acknowledgments

The authors would like to thank Saudi Aramco for funding and Dr. James Bennett for scientific discussion and advice.

Nomenclature and units

$[A]$: catalyst concentration , mol m^{-3}

C_i: H_2 concentration in ethanol at the ethanol-H_2 bubble interface , mol m^{-3}

D: the diffusivity of solute A in solvent B , m^2 s^{-1}

D_{AB}: liquid diffusivity of solute A , m^2 s^{-1}

De : effective diffusivity, m^2 s^{-1}

d_p: diameter of catalyst particle, m

d_v: equivalent volume diameter, $d_v = (6V_p/\pi)^{1/3}$, m

Fr_L: liquid Froude number, $Fr_L = V_{SL}^2/gd_v$

G_l: superficial mass velocity of liquid, kg m^{-2} s^{-1}

g: gravitational constant, m s^{-2}

K : specific reaction rate, s^{-1}

K_1, K_2: equilibrium constants, m^3 mol^{-1}

K_c: mass transfer coefficient, m s^{-1}

k', k'': rate constants, m^3 mol^{-1} s^{-1}

M_B: the molecular weight of the solvent

Mo_L: liquid Morton number, $Mo_L = g\,\mu_L^4/\rho_L\sigma_L^3$

m : catalyst loading, kg of catalyst / m^3 of solution.

P: concentration of hydrogen in the solution, mol m^3

R : Pellet radius, m

R_A: rate of reaction per volume of solution, mol / (m^3 of solution · s)

Re: Reynolds Number, $Re = G_l d_p/\mu_l$

r_b: resistance to gas absorption, s

r_{cr}: specific combined resistance to internal diffusion, reaction, and external diffusion, kg cat · s / m^3

$[S]$: substrate concentration, mol l^{-1}

S_a : surface area per unit mass of catalyst, m^2 g^{-1}

Sc: Schmidt number, $Sc = vD_{AB}{}^{-1}$

Sh: Sherwood number, $Sh = K_c d_p \alpha / D_{AB}$

T: the temperature, K

v: kinematic viscosity, m^2 s^{-1}

V_A: the molecular volume of the solute, m^3 mol^{-1}

V_{SL}: superficial liquid velocity, m s^{-1}

α : fraction of external surface that is wetted

ε_B: porosity of the alumina particle bed

η : internal effectiveness factor

μ: the viscosity of the solution, Pa · s

μ_L, μ_l: liquid viscosity, Pa · s

ρ_c : density of catalyst particle, kg m^{-3}

ρ_L: liquid density, kg m^{-3}

σ_L: liquid surface tension, kg s^{-2}

ϕ : Thiele modulus

$\emptyset_B$: the association factor for the solvent

References

[1] A. Baiker, J. Mol. Catal. A Chem. 115 (1997) 473-493.
[2] A. Crosman, W.F. Hoelderich, J. Catal. 232 (2005) 43–50.
[3] H. Blaser, B. Pugin, F. Spindler, J. Mol. Catal. A Chem. 231 (2005) 1–20.
[4] C. Simons, U. Hanefeld, I.W.C.E. Arends, R.A. Sheldon, T. Maschmeyer, Chem. Eur. J. 10 (2004) 5829-5835.
[5] W.P. Hems, P. McMorn, S. Riddel, S. Watson, F.E. Hancocka, G.J. Hutchings, Org. Biomol. Chem. 3 (2005) 1547-1550.
[6] F. Quignard, A. Choplin, in: J.A. McCleverty, T.J. Meyer (Eds.), Comprehensive Coordination Chemistry II, Elsevier Ltd. Oxford, 2003, pp. 445-446.
[7] H. Blaser, B. Pugin, M. Studer, in: D.E. De Vos, I.F.J. Vankelecom, P.A. Jacobs (Eds.), Chiral Catalyst Immobilization and Recycling, Wiley-VCH. Germany, 2000, pp. 9-11.
[8] R.L. Augustine, P. Goel, N. Mahata, C. Reyes, S.K. Tanielyan, J. Mol. Catal. A Chem. 216 (2004) 189–197.
[9] R.L. Augustine, S.K. Tanielyan, N. Mahata, Y. Gao, A. Zsigmond, H. Yang, Appl. Catal. A Gen. 256 (2003) 69–76.
[10] http://www.manufacturingchemist.com/technical/article_page/Turn_batch_to_continuous_processing/54954, accessed on 05/07/2010.
[11] E. Toukoniitty, P. Mäki-Arvela, A. Kalantar Neyestanaki, T. Salmi, D.Yu. Murzin, Appl. Catal. A Gen. 235 (2002) 125–138.
[12] F. Turek, R.K. Chakrabarti, R. Lange, R. Geike, W. Flock, Chem. Eng. Sci. 38 (1983) 275-283.
[13] P. Gallezot, N. Nicolaus, G. Flèche, P. Fuertes, A. Perrard, J. Catal. 180 (1998) 51-55.
[14] A.R. Bogdan, B.P. Mason, K.T. Sylvester, D.T. McQuade, Angew. Chem. Int. Ed. 46 (2007) 1698-1701.
[15] G.P. Stahly, R.M. Starrett, in: A.N. Collins, G.N. Sheldrake, J. Crosby (Eds.), Chirality in Industry II, Wiley, New York, 1997, p. 19.
[16] R.A. Sheldon, Chirotechnology: Industrial Synthesis of Optically Active Compounds, Marcel Dekker, New York, 1993, p. 347.
[17] S.N. Wang and F. Kienzle, Org. Proc. Res. Dev. 2 (1998) 226–229.
[18] B. Hermán, G. Szőllősi, F. Fülöp, M. Bartók, Appl. Catal. A Gen. 331 (2007) 39–43.
[19] N. Künzle, T. Mallat, A. Baiker, Appl. Catal. A Gen. 238 (2003) 251–257.
[20] N. Künzle, J.-W. Soler, T. Mallat, A. Baiker, J. Catal. 210 (2002) 466–470.
[21] E. Toukoniitty, P. Mäki-Arvela , A.K. Neyestanaki, T. Salmi , R. Sjöholm, R. Leino , E. Laine , P.J. Kooyman, T. Ollonqvist, J. Väyrynen, Appl. Catal. A Gen. 216 (2001) 73–83.
[22] J.M. Winterbottom, Z. Khan, S. Raymahasay, G. Knight, N. Roukounakis, J. Chem. Technol. Biotechnol. 75 (2000) 1015-1025.
[23] J.J. Heiszwolf, L.B. Engelvaart, M.G. van den Eijnden, M.T. Kreutzer, F. Kapteijn, J.A. Moulijn, Chem. Eng. Sci. 56 (2001) 805-812.
[24] F. Gao, K.P. Ng, C. Li, K.I. Krummel, A.D. Allian, M. Garland, J. Catal. 237 (2006) 49-57.
[25] K. Inoguchi, T. Morimoto, K. Achiwa, J. Organomet. Chem. 370 (1989) C9-Cl2.
[26] Y. Sun, R.N. Landau, J. Wang, C. LeBlond, D.G. Blackmond, J. Am. Chem. Soc. 118 (1996) 1348-1353.
[27] A. Berger, R.F. de Souza, M.R. Delgado, J. Dupont, Tetrahedron Asymmetry 12 (2001) 1825–1828.
[28] N. Pestre, V. Meille, C. Bellefon, J. Mol. Catal. A Chem. 252 (2006) 85–89.
[29] H.S Fogler, Elements of Chemical Reaction Engineering, third ed., Prentice-Hall, Inc. New Jersey, 1999.

[30] J.A.M. Brandts and P. H. Berben, Org. Process Res. Dev. 7 (2003) 393-398.
[31] J.A. Osborn, F.H. Jardine, J.F. Young, G. Wilkinson, J. Chem. Soc. A (1966) 1711 – 1732.
[32] C.V. Rode, P.R. Tayade, J. M. Nadgeri,, R. Jaganathan, and, R. V. Chaudhari, Org. Process Res. Dev. 10 (2006) 278-284.
[33] J. S. Milano-Brusco, M. Schwarze, M. Djennad, H. Nowothnick, R. Schomacker, Ind. Eng. Chem. Res. 47 (2008) 7586–7592.
[34] P.A. Ramachandran and R.V Chaudhari, Three- Phase Catalytic Reactors, Gordon and Breach Science Publishers Ltd, New York, 1983, p.202.
[35] V. Nedovic, R. Willaert (Eds.), Fundamentals of Cell Immobilisation Biotechnology, Kluwer Academic Publishers, Netherlands, 2004, p.418.
[36] B. Pugin, J. Mol. Catal. A Chem. 107 (1996) 273-279.
[37] E.E. Jacobsen, L.S. Andresen, T. Anthonsen, Tetrahedron Asymmetry 16 (2005) 847-850.
[38] S. Coleman-Kammula, E.T. Duim-Koolstra, J. Organomet. Chem. 246 (1983) 53-56.
[39] H.E.B. Lempers, R.A. Sheldon, J. Catal. 175 (1998) 62-69.
[40] B.A. Wilhite, X. Huang, M.J. McCready, A. Varma, Ind. Eng. Chem. Res. 42 (2003) 2139-2145.
[41] J.G. Boelhouwer, H.W. Piepers, A.A.H. Drinkenburg, Chem. Eng. Sci. 57 (2002) 3387-3399.
[42] C.J. Lebigue, F. Augier, H. Maffre, A.M. Wilhelm, H. Delmas, Ind. Eng. Chem. Res. 48 (2009) 6811–6819.
[43] J.M. Winterbottom, M.B. King (Eds.), Reactor Design for Chemical Engineers, Stanley Thornes, Cheltenham, 1999, pp.362-373.
[44] J.M. Coulson, J.F. Richardson, Coulson & Richardson's Chemical Engineering, sixth ed., Butterworth-Heinemann, Oxford, 1999.
[45] A.K. Mogalicherla, G. Sharma, D. Kunzru, Ind. Eng. Chem. Res. 48 (2009) 1443–1450.
[46] M. Herskowitz, R.G. Carbonell, J.M. Smith, AIChE J. 25 (1979) 272-283.

List of Figures

List of Graphics (Schemes)

List of Tables

Table 1:
Chemicals and solvents used in this study

Material	Supplier	Specification/treatment
Phosphotungstic acid (PTA)	Sigma Aldrich, UK	Used as received
Powder alumina support (neutral γ-alumina), 97%	Strem Chemicals, Inc, UK	Surface area 258×10^3 $m^2\ kg^{-1}$
Trilobe alumina support	Johnson Matthey, UK	Surface are 149×10^3 $m^2\ kg^{-1}$
Dimetyl itaconate (DMI), 97%	ACROS ORGANICS, USA	Used as received
[Rh((R,R)-Me-DuPhos)(COD)]BF_4, 98+%	Strem Chemicals, Inc, USA	

Table 2:
Characteristics of powder and trilobe alumina supports

Support	BET area ($m^2\ g^{-1}$)	Average pore size (nm)	Pore volume ($cm^3\ g^{-1}$)
Powder alumina	258	9.4	0.6
Trilobe alumina	149	19.3	0.72

Table 3:
Results from testing different concentrations of DMI in the shake-flask reactor with powdered immobilised catalyst.[a]

DMI concentration ($\times 10^3$ mol m^{-3})	Substrate/catalyst molar ratio	Initial reaction rate[b]	% Conversion	TOF (h^{-1})	% ee
0.01	9	0.005	97	9	97
0.03	26	0.018	98	25	96
0.08	61	0.035	99.9	60	96
0.16	122	0.038	100	99	97
0.26	196	0.047	33	45	94
0.412	311	0.023	19	31	93

[a] In 15 ml (15×10^{-6} m^3) ethanol, 20 °C (293.15 K) temperature, atmospheric pressure (101317 Pa), 20 µmol (20×10^{-6} mol) of catalyst precursor complex, H_2 flow of 100 ml min^{-1} (1.7×10^{-6} m^3 s^{-1}) and shaking speed of 200 rpm.
[b] mol DMI / (m^3 of solution · s);calculated after 10 minutes from the start of the reaction

Table 4:
Rate and equilibrium constants for the hydrogenation of DMI in the shake-flask and trickle-bed reactors.[a]

	k'/m^3 mol^{-1} s^{-1}	k''/ m^3 mol^{-1} s^{-1}	K_1/m^3 mol^{-1}	K_2 / m^3 mol^{-1}
Shake-flask reactor	0	1.26×10^{-6}	201×10^{-3}	196
TBR	0	2.46×10^{-6}	943×10^{-3}	196

[a] values of constants were predicted using excel solver.

Table 5:
Comparison of powder and trilobe alumina supports in the shake-flask reactor.[a]

support	Surface area (m^2 kg^{-1})	Initial reaction rate[b]	% Conversion	% ee	Time (min)
Powder alumina	258×10^3	0.032	99.9	96	72
Trilobe alumina	149×10^3	0.015	97	97	180

[a] In 15 ml (15×10^{-6} m^3) ethanol, 20 °C (293.15 K) temperature, atmospheric pressure (101317 Pa), substrate/ catalyst ratio:60, 20 µmol (20×10^{-6} mol) of catalyst precursor complex, H_2 flow of 100 ml min^{-1} (1.7×10^{-6} m^3 s^{-1}) and shaking speed of 200 rpm.
[b] mol DMI / (m^3 of solution · s).

Table 6:
Optimizing catalyst bed by testing different catalyst loadings.[a]

Catalyst loading (kg complex/kg support)	Initial Reaction rate[b]	% Conversion	% ee	Time (min)
12.2×10^{-3}	6.7×10^{-3}	70	80	330
4.4×10^{-3}	28×10^{-3}	99	95	70

[a] In 15 ml (15×10^{-6} m^3) ethanol, 20 °C (293.15 K) temperature, atmospheric pressure (101317 Pa), 1.3×10^{-3} mole DMI, , H_2 flow of 100 ml min^{-1} (1.7×10^{-6} m^3 s^{-1}) and liquid flow of 20 ml min^{-1} (3.3×10^{-7} m^3 s^{-1}). Complexes were immobilised onto 2.7×10^{-3} kg of trilobe alumina support.
[b] mol DMI / (m^3 of solution · s).

Table 7:
Results from testing different concentrations of DMI in the TBR.[a]

DMI concentration (x 10^3 mol m^3)	Substrate/catalyst molar ratio	Cycle	Initial reaction rate[b]	% Conversion	TOF (h^{-1})	% ee
0.105	85	1	0.029	99	85	95
		2	0.024	97		96
		3	0.008	17		99.9
0.170	128		0.029	97	82	86
0.237	179		0.032	97	79	87
0.300	223	1	0.043	99	114	99.9
		2	0.018	52		94

[a] In 15 ml (15×10^{-6} m^3) ethanol, 20 °C (293.15 K) temperature, atmospheric pressure (101317 Pa), 20 µmol (20×10^{-6} mol) of catalyst precursor complex supported on 2.7×10^{-3} kg of trilobe alumina, H_2 flow of 100 ml min^{-1} (1.7×10^{-6} m^3 s^{-1}) and liquid flow of 20 ml min^{-1} (3.3×10^{-7} m^3 s^{-1}) .
[b] mol DMI / (m^3 of solution · s); calculated after 30 minutes from the start of the reaction.

Table 8:
Effect of gas and liquid flow rates in the TBR.[a]

entry	Liquid flow rate ($\times 10^{-7}$ m^3 s^{-1})	Gas flow rate ($\times 10^{-6}$ m^3 s^{-1})	Initial reaction rate[b]	% Conversion	% ee
1	3.3	0.83	0.040	98	87
2	3.3	1.7	0.043	99	99.9
3	3.3	3.3	0.048	97	94
4	1.7	1.7	0.022	96	93
5	2.5	1.7	0.032	96	98
6	3.3	1.7	0.043	99	99.9

[a] In 15 ml (15×10^{-6} m^3) ethanol, 20 °C (293.15 K) temperature, atmospheric pressure (101317 Pa), 20 µmol (20×10^{-6} mol) of catalyst precursor complex supported on 2.7×10^{-3} kg of trilobe alumina, substrate/catalyst molar ratio: 223.
[b] mol DMI / (m^3 of solution · s); [entry 1,2 and 3] : calculated after 10 minutes from the start of the reaction; [entry 4,5 and 6]: calculated after 60 minutes from the start of the reaction.

Table 9:
Wetting efficiencies and mass transfer coefficients of different liquid flow rates in TBR.
[a]

Liquid flow rate ($m^3\ s^{-1}$)	Liquid superficial velocity ($m\ s^{-1}$)	Froude number (Fr_L)	Reynolds number (Re)	Wetting efficiency	Mass transfer coefficient ($\times 10^{-4}\ m\ s^{-1}$)
1.7×10^{-7}	0.00589	0.00124	8.448	0.915	0.744
2.5×10^{-7}	0.00883	0.00279	12.673	0.936	1.158
3.3×10^{-7}	0.01178	0.00497	16.897	0.949	1.590

[a] Diffusivity of H_2 into ethanol was calculated using correlation (5) to be $7.48 \times 10^{-9}\ m^2\ s^{-1}$; Sc number was calculated to be 203.246; Mo_L was calculated to be 1.62×10^{-9}; porosity of bed (ε_B) = 0.634.

Figure(s)
Click here to download high resolution image

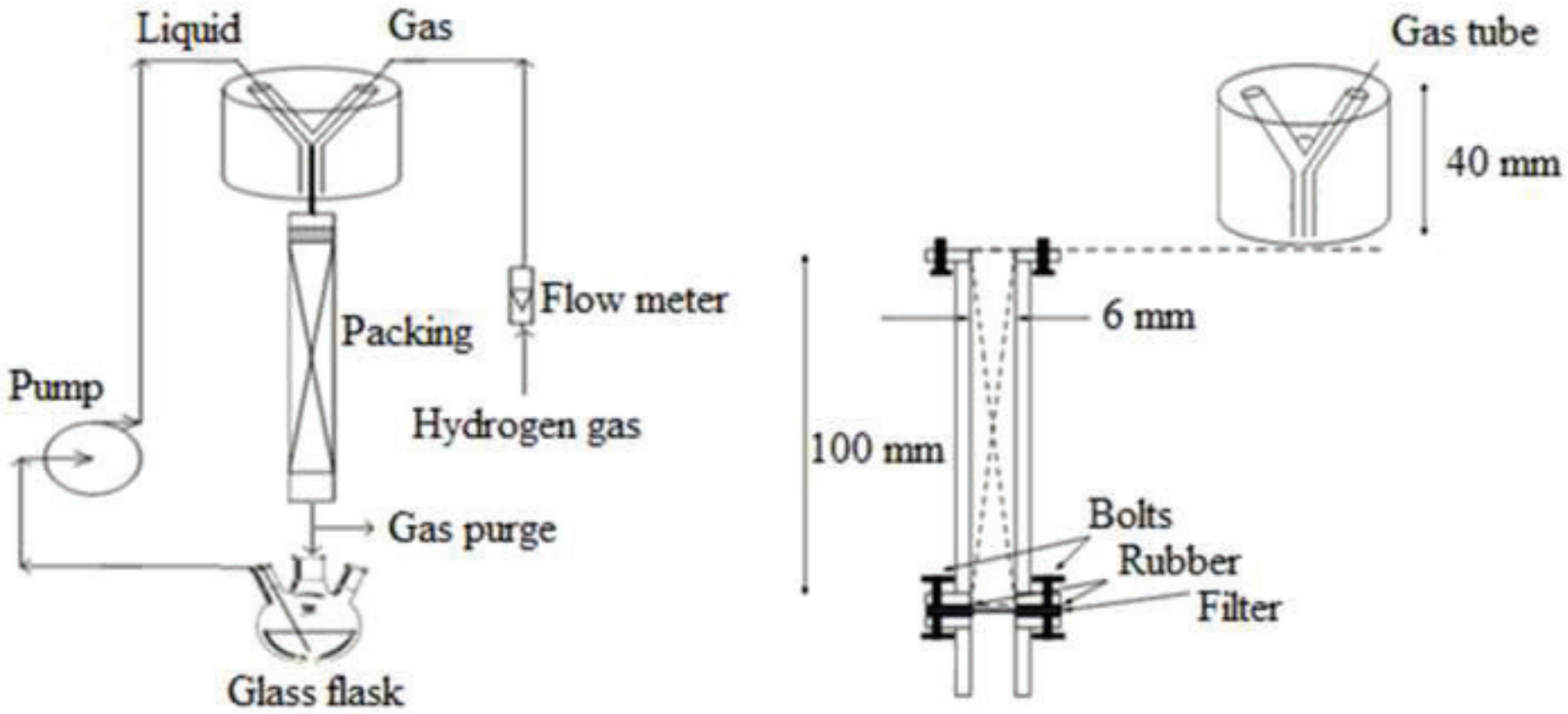

Figure(s)
Click here to download high resolution image

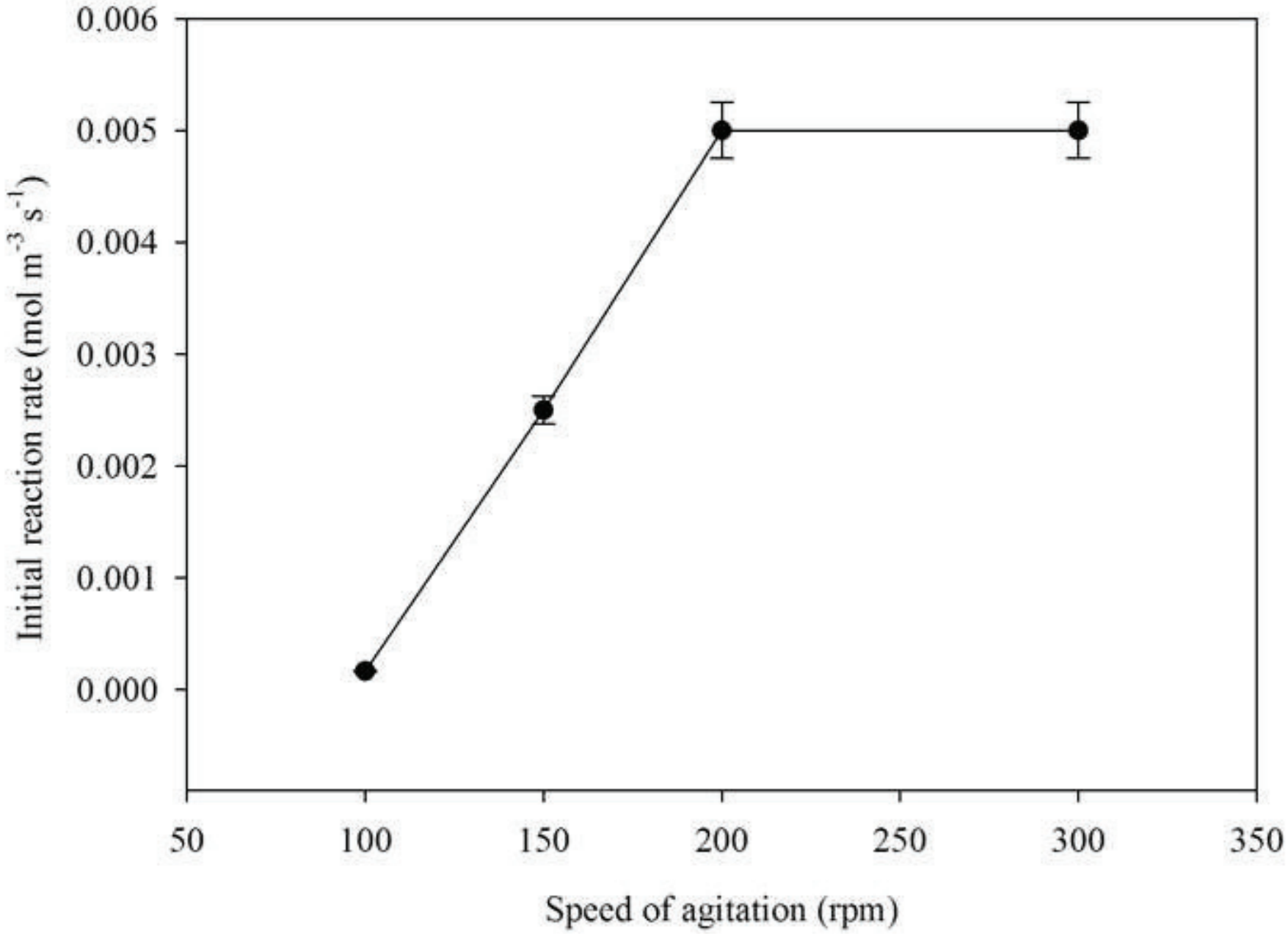

Figure(s)
Click here to download high resolution image

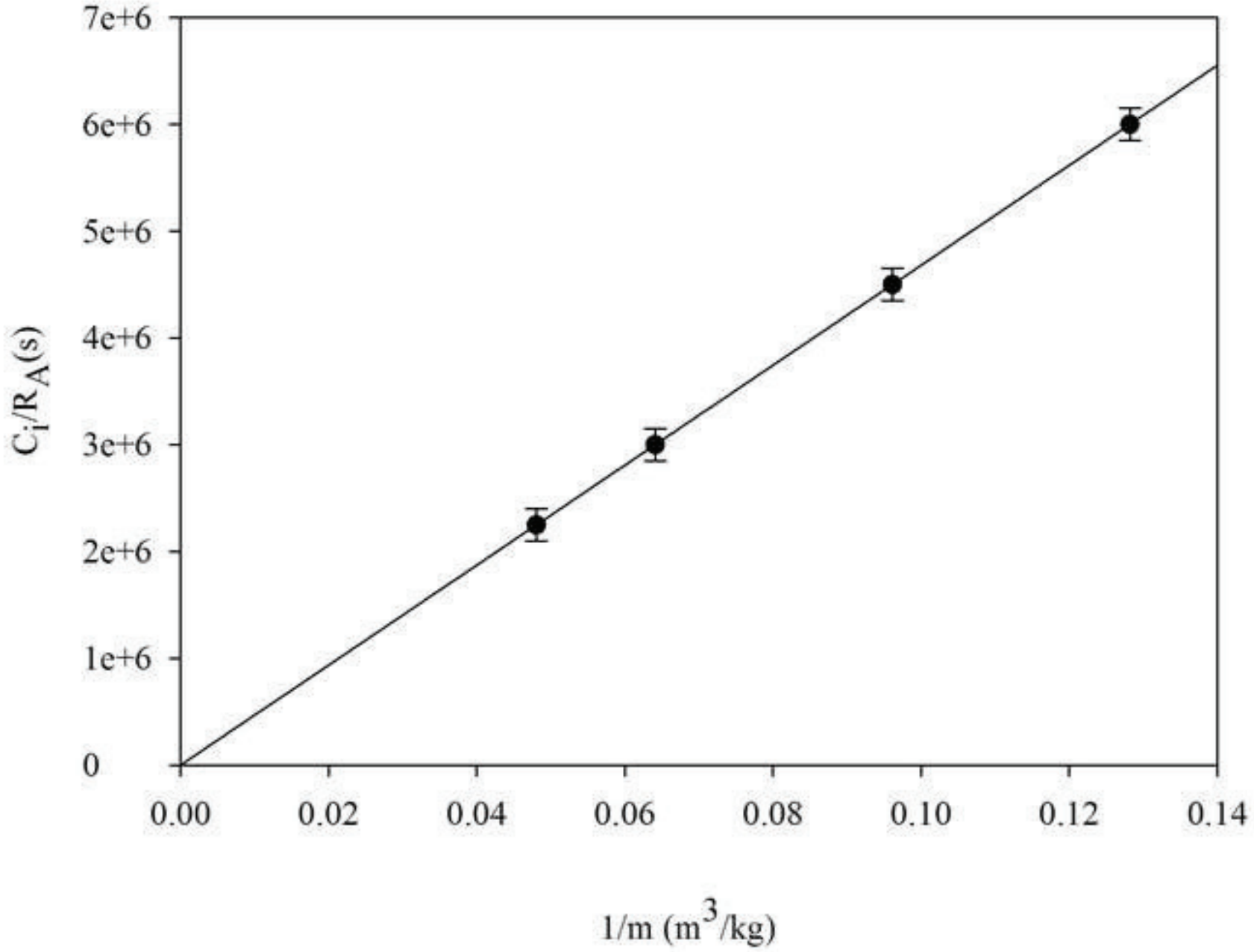

Figure(s)
Click here to download high resolution image

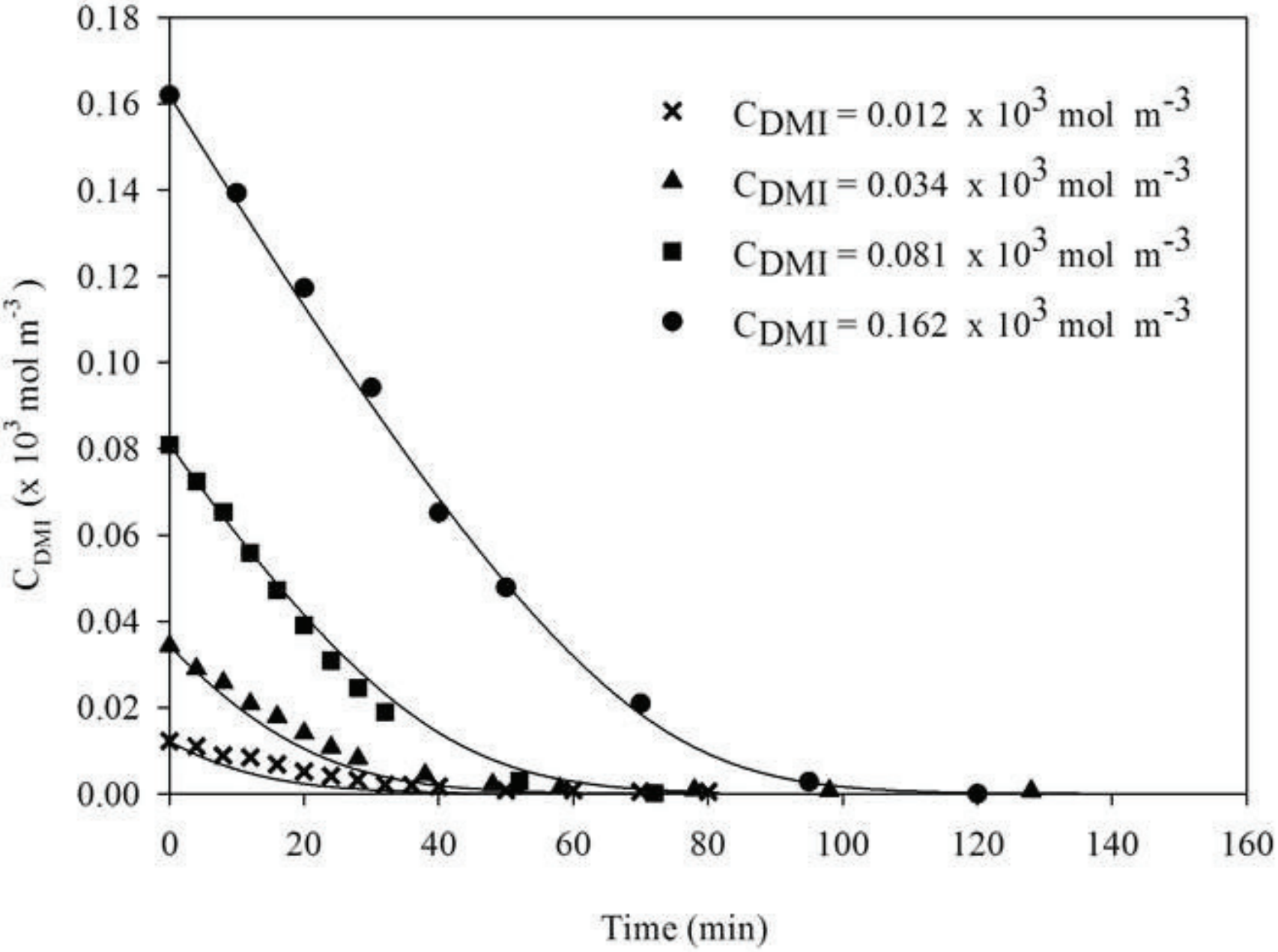

Figure(s)
Click here to download high resolution image

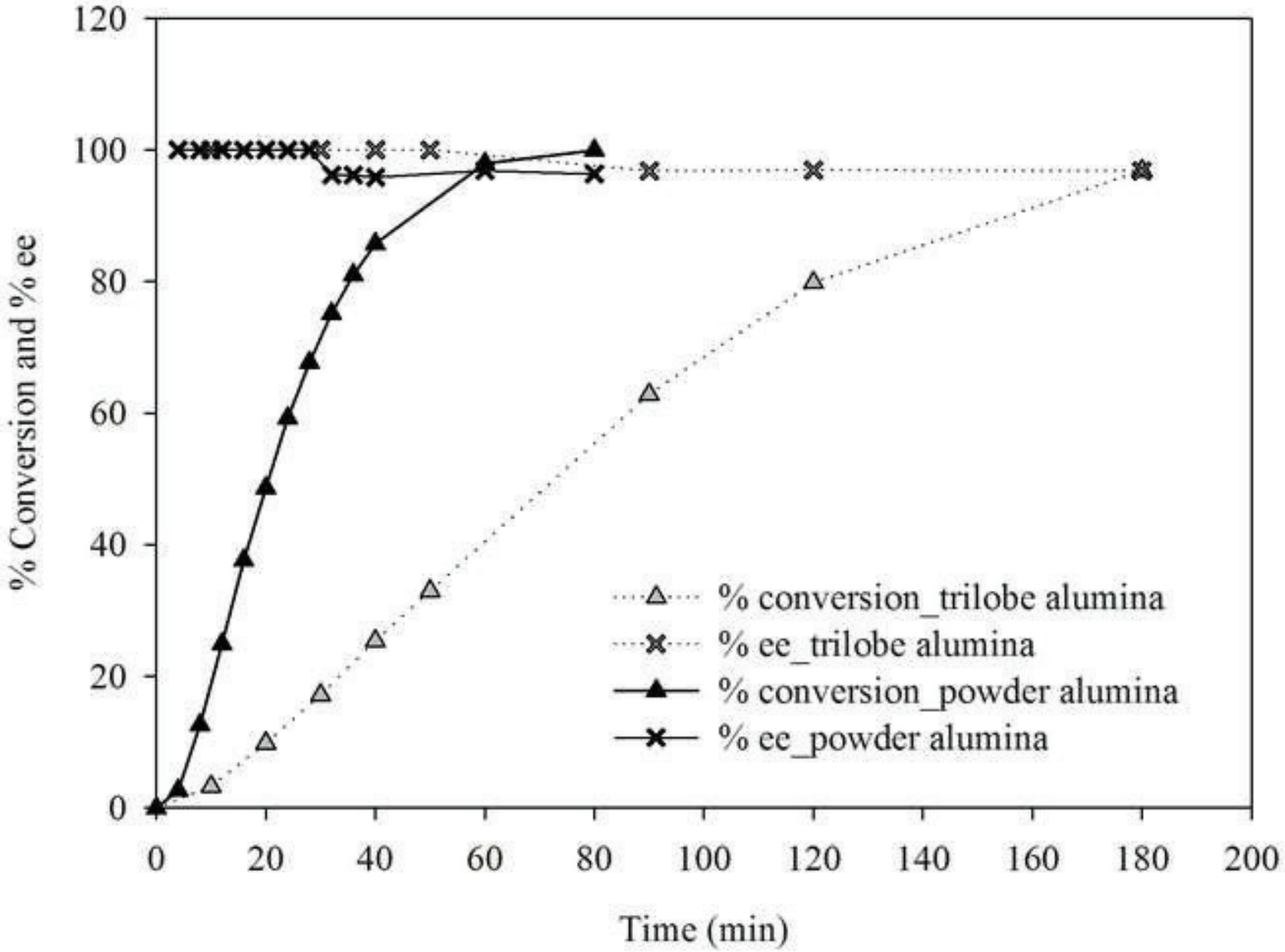

Figure(s)
Click here to download high resolution image

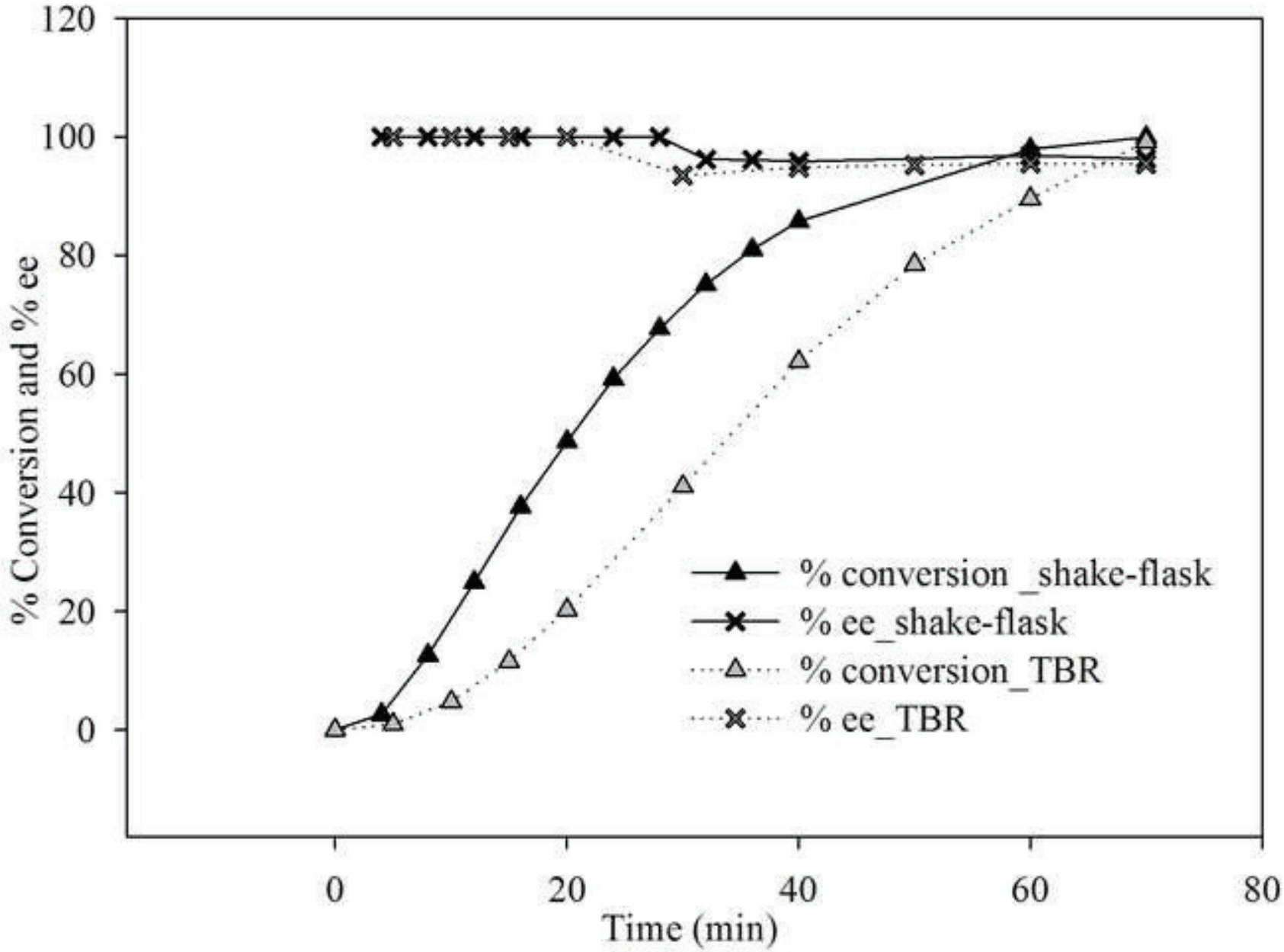

Figure(s)
Click here to download high resolution image

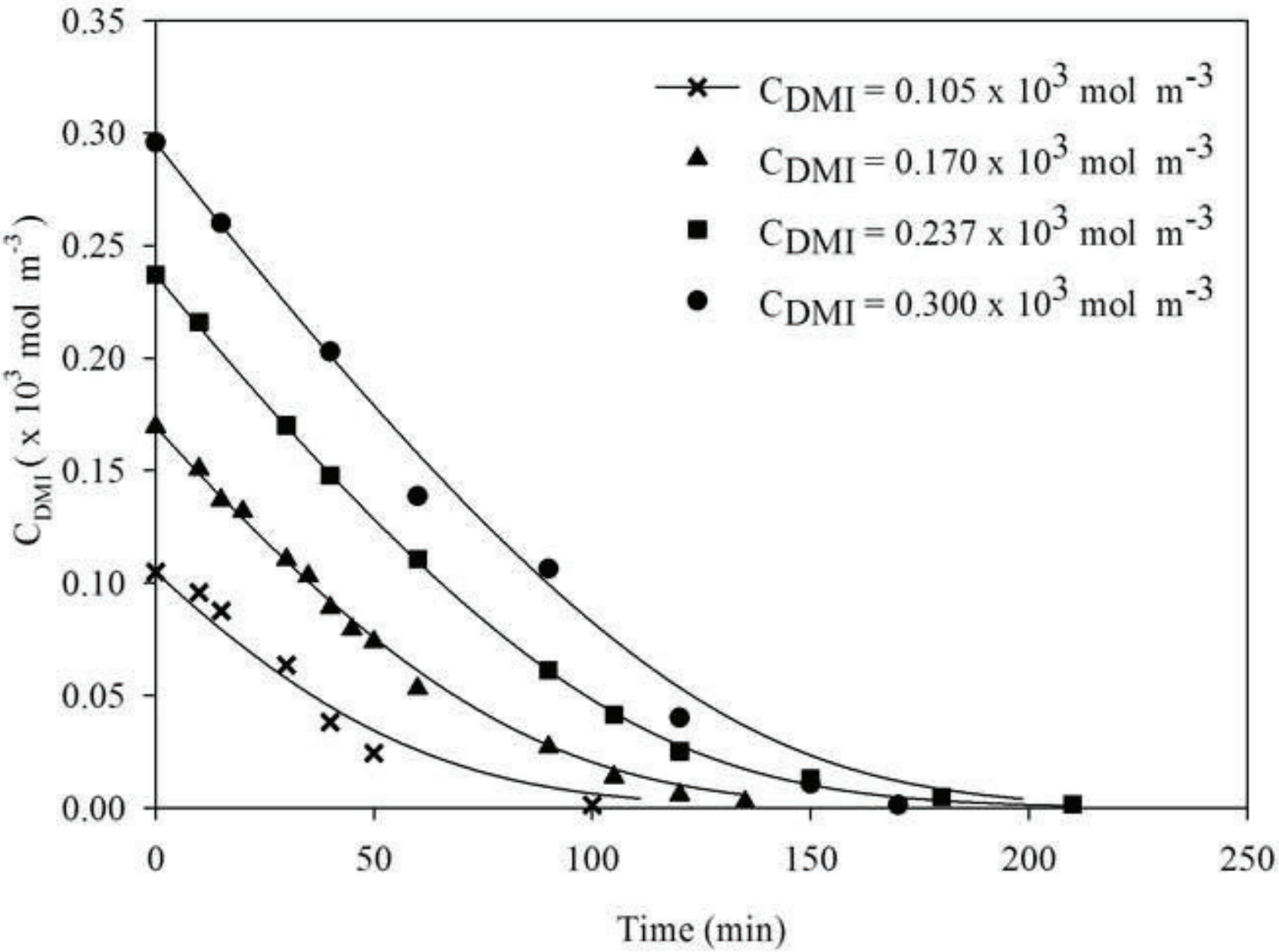

Figure(s)
Click here to download high resolution image

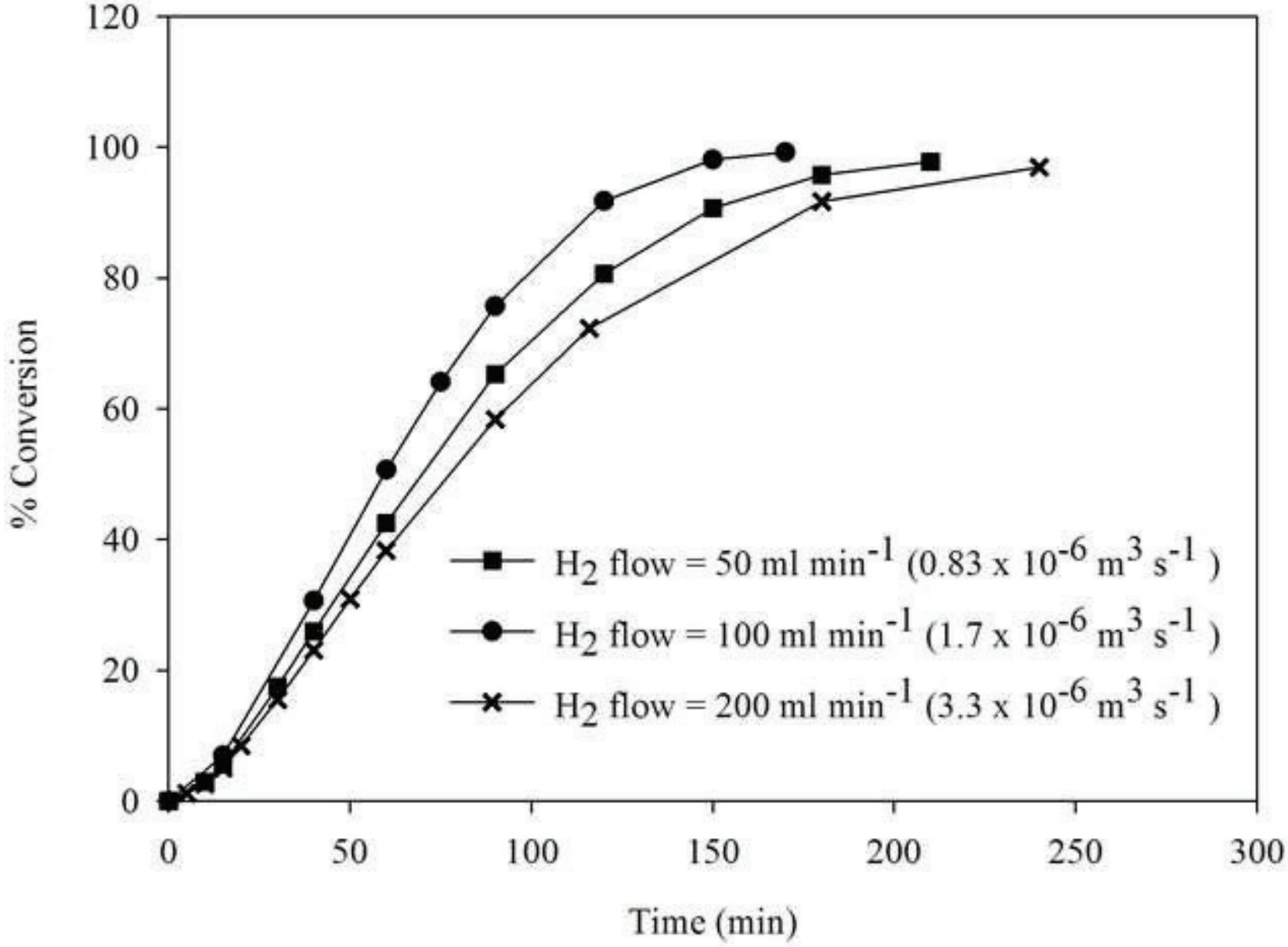

Figure(s)
Click here to download high resolution image

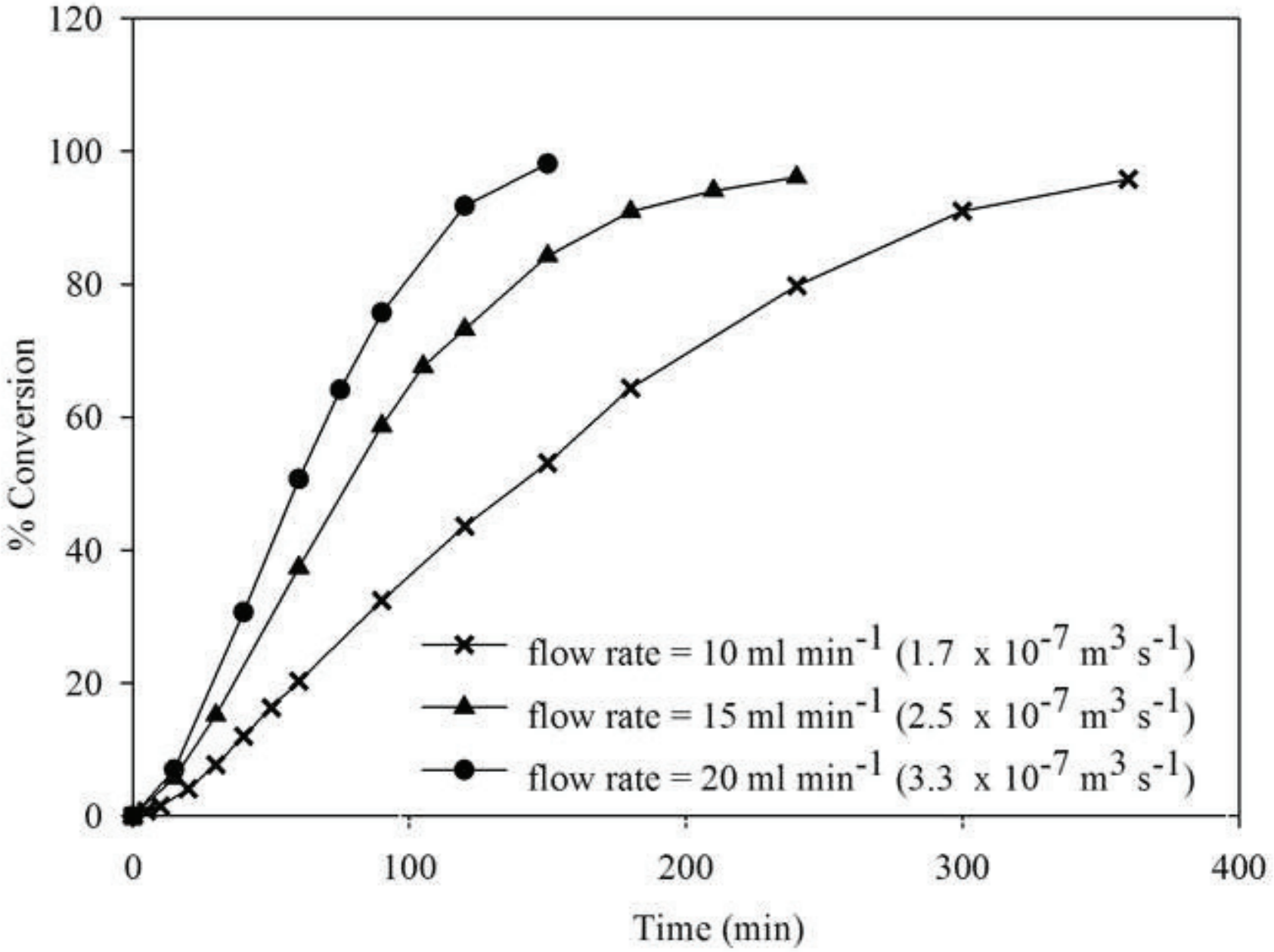

Figure(s)
Click here to download high resolution image

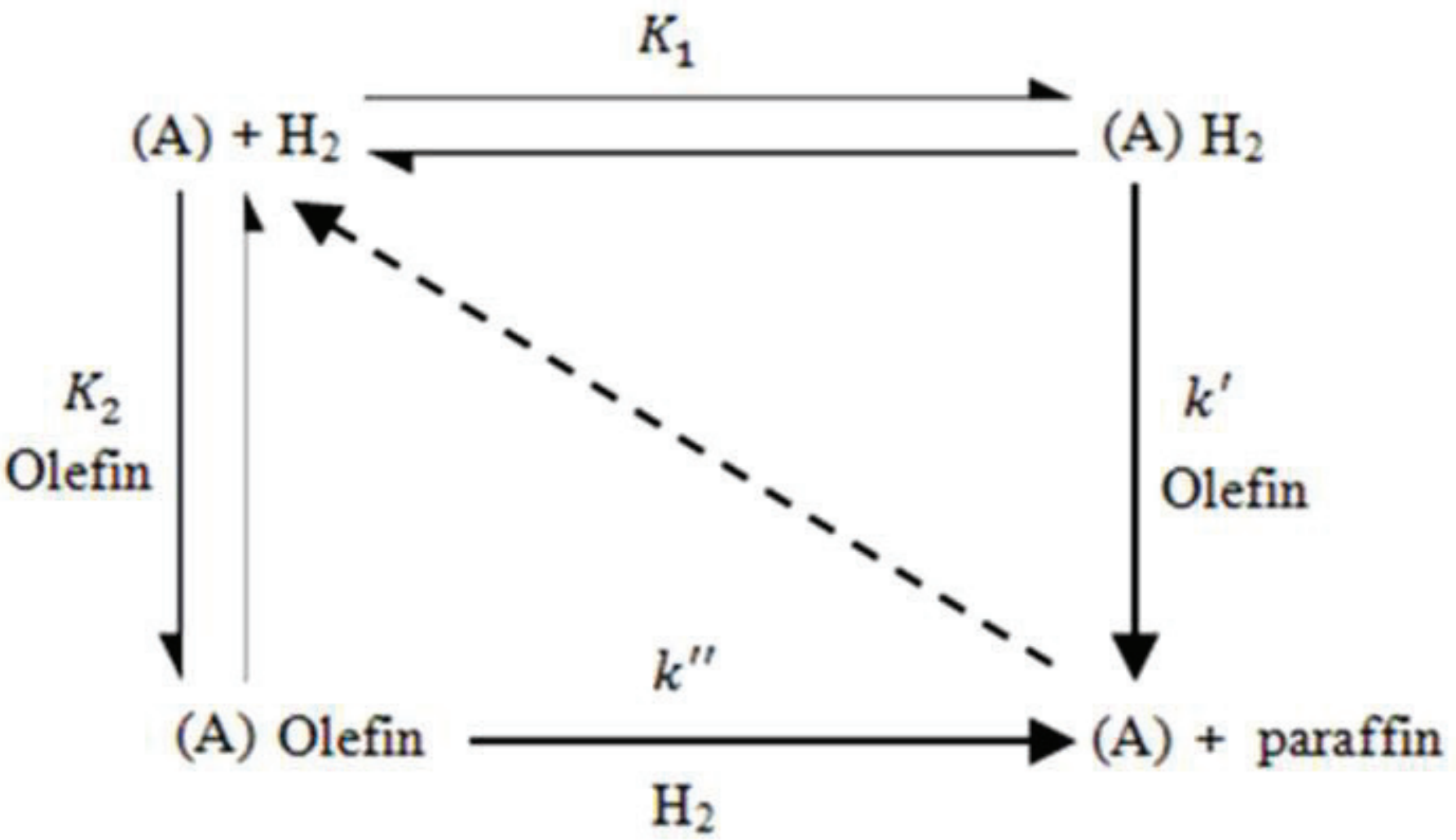

Figure(s)
Click here to download high resolution image